arXiv:cond-mat/0506799v1 [cond-mat.soft] 30 Jun 2005

Deformation of Silica Aerogel During Fluid Adsorption

Tobias Herman,* James Day, and John Beamish
Department of Physics, University of Alberta, Edmonton, Alberta, Canada, T6G 2J1

(Dated: February 2, 2008)

Aerogels are very compliant materials — even small stresses can lead to large deformations. In this paper we present measurements of the linear deformation of high porosity aerogels during adsorption of low surface tension fluids, performed using a Linear Variable Differential Transformer (LVDT). We show that the degree of deformation of the aerogel during capillary condensation scales with the surface tension, and extract the bulk modulus of the gel from the data. Furthermore we suggest limits on safe temperatures for filling and emptying low density aerogels with helium.

PACS numbers: 61.43.Gt, 62.20.Fe, 68.03.Cd

I. INTRODUCTION

Porous media have large surface areas, and consequently interfacial energy contributes significantly to their behavior. The energetic cost of the solid-vacuum interface in an empty porous medium produces a stress on the matrix; when fluid is adsorbed the interfacial energy may decrease, reducing the stress on the matrix and allowing it to expand. As more fluid is adsorbed, liquid begins to capillary condense, creating a large number of curved liquid-vapor interfaces throughout the sample. The energy of these liquid-vapor interfaces creates another stress which may result in contraction of the porous medium. The expansion of a porous medium upon adsorption of fluids has been observed in a number of systems over the past century[1,2,3,4,5]; contraction has also been observed[6].

Aerogels present a somewhat different system than the denser porous media since they are composed of a very low density network of silica strands, often with total porosities over 95%. As such they have very low elastic constants, with most elastic strain being accounted for by the bending and twisting of the strands[7] rather than compression of the silica making up those strands. Therefore the effective elastic constants for aerogels can be orders of magnitude smaller than bulk silica, and aerogels are very sensitive to small changes in stress caused by interfacial energy.

A porous medium exposed to vapor at low pressure collects a thin film on the surface of the pores. As vapor pressure is increased this film thickens slowly until the fluid suddenly capillary condenses at some pressure below bulk saturation. Liquid invades the pores over a narrow pressure range, driven by the pressure difference across the curved liquid-vapor interface within the pores. While this pressure difference may be small compared to the elastic constants of typical solids, it can be comparable to the bulk moduli of low density aerogels. In such a situation the forces generated by the liquid-vapor interface during capillary condensation can deform the medium measurably. The capillary forces generated by water in aerogel are sufficient to completely crush the gel — a fact known to anyone who has accidentally gotten a drop of water on a hydrophilic aerogel.

Deformation of aerogel during liquid nitrogen adsorption and desorption has been measured by Reichenauer and Scherer[8,9] for some aerogels with densities between $150 - 240 \frac{kg}{m^3}$ (porosities between 88% and 93%) with a view to incorporating the distortion of the aerogel into existent methods of determining pore sizes from N_2 adsorption isotherms. The aerogels in that study had Young's moduli of 3.8MPa (implying a bulk modulus of about 2MPa) and greater, much larger than the aerogels in this study. Their aerogels exhibited large changes in volume during capillary condensation, and were permanently damaged by the process. They also observed that information about the elastic properties of their samples could be extracted from the isotherms.

The high surface tension and large contact angle of mercury prevents it from entering the pores of aerogels when placed in a mercury porosimeter. In this case the surface tension is so great that when the aerogel is subjected to large pressures it plastically deforms[10,11], down to a fraction of its original volume.

Shen and Monson performed a Monte Carlo study of fluid adsorption in a flexible porous network which resembled a high porosity aerogel[12]. Their simulated adsorption isotherms showed that the flexibility of the network had a large effect on the adsorption isotherms, and that the network exhibited a large volumetric change, especially during desorption.

Aerogels are widely used as a method to introduce a "quenched impurity" into a fluid, often with the goal of exploring the effect of fixed disorder on fluid order and phase transitions. Experiments with quantum fluids have included ^{3}He[13,14], ^{4}He[15,16], and ^{3}He-^{4}He mixtures[17,18,19]. Liquid crystals in aerogels[20] have also been widely studied. Implicit in all of these studies is an assumption that the structure of the aerogel is not affected by the fluid within its pores, nor is the aerogel altered during filling or emptying. While studying the temperature and porosity dependence of adsorption isotherms in aerogels[21], we noticed that the isotherm shapes might be showing effects from the deformation of the aerogel by the adsorbed fluid. This study is aimed at quantifying the degree of aerogel deformation during helium adsorption at a variety of temperatures.

We have measured the macroscopic linear strain in two different low density aerogels during adsorption and desorption of low surface tension fluids. Our measurements included an isotherm of neon adsorbed in a $51\frac{kg}{m^3}$ ($\sim 98\%$ porosity) silica aerogel at 43K and several isotherms of helium adsorbed in a $110\frac{kg}{m^3}$ (95% porosity) silica aerogel at temperatures from 2.4K to 5.0K. At these temperatures the fluid surface tensions were small, but the low elastic constants of the aerogels allowed a significant deformation nevertheless. The compression of the aerogel was greatest during desorption. From the isotherms we show that the degree of compression during capillary condensation within the aerogel is directly related to the surface tension of the adsorbate. Furthermore, the bulk modulus of the aerogel was extracted from the adsorption and desorption isotherms.

The compression due to capillary condensation has not previously been studied in such compliant materials. By using high porosity aerogels, we were able to directly observe, for the first time, the deformation associated with low surface tension fluids like helium. By making measurements very slowly, we avoided rate dependent effects and were able to study the hysteresis between compression during filling and emptying of aerogels. Our measurements extended close to helium's critical point, which allowed us to vary the surface tension over a wide range compared to previous measurements, which used nitrogen and much more rigid samples. From our results, it is clear that the deformation associated with surface tension must be taken into account when interpreting adsorption isotherms and to avoid damage when filling high porosity aerogels.

II. EXPERIMENTAL METHOD

The aerogel samples were synthesized in our lab from tetramethyl orthosilicate (TMOS) using a standard one-step base catalyzed method followed by supercritical extraction of the methanol solvent[22]. The two aerogels studied had densities of $110\frac{kg}{m^3}$ and $51\frac{kg}{m^3}$, corresponding to porosities of 95% and slightly less than 98% respectively. They are referred to as aerogels "B110" and "B51" throughout this paper. Both aerogel samples were cut into cylinders about 1cm long. B51, used in the first experiment, was about 1.2cm in diameter — it equilibrated so slowly that it took weeks to measure a single isotherm. To reach thermal equilibrium more quickly, a smaller sample of B110 (4mm in diameter) was used for the second experiment.

Our linear variable differential transformer (LVDT) allowed us to make high precision, non-contact measurements of the relative position of a cylindrical ferromagnetic core and a set of primary and secondary coils[30]. The response of the LVDT was highly temperature dependent, and room temperature calibrations were not used to interpret the low temperature data. In the liquid helium cryostat it was possible to make a direct calibration of the LVDT, but for measurements with neon an approximate calibration had to be computed from the adsorption isotherm itself (as will be explained later).

Two experimental cells were used over the course of this experiment to accommodate the two different aerogel samples. Both cells were made of copper and had the same general layout, with the LVDT core supported about 2cm above the sample by a thin brass rod. The support was kept in contact with the sample by gravity, and the cells kept upright once assembled. The initial position of the external LVDT coils relative to the core was controlled through set screws.

In our initial experiment neon was admitted to the experimental cell containing B51 in volumetric shots from a room temperature gas handling system, and pressure measurements were made with a room temperature gauge[31]. Cooling was provided by a Gifford-McMahon closed cycle refrigerator; the temperature was controlled to ±1mK using a platinum resistance thermometer and a thick-film heater mounted directly on the cell.

In the second set of measurements, on helium in B110, the fluid condensation into the system was controlled by stepping the pressure in the cell through the use of a low temperature pressure regulation ballast[21]. This second method did not provide information on the absolute quantity of fluid adsorbed by the aerogel but ensured long term pressure stability. A Straty-Adams[23] type capacitive pressure gauge was used for low temperature *in situ* pressure measurement. The cell was mounted on a liquid helium cryostat; the temperature was controlled to $\pm 50\mu$K using a germanium resistive thermometer and thick-film heater mounted directly on the cell.

III. NEON AT 43K IN B51

The adsorption and desorption isotherms for neon at 43K in B51 are shown in Fig. 1a. Note that neon at 43K is very close to its critical point ($T_c \sim 44.5$K, $P_c \sim 2.7$MPa, $\rho_c \sim 485\frac{kg}{m^3}$). As such, it has a very low surface tension (at 43K neon has the same surface tension as liquid helium does at 3.7K) and its liquid and vapor densities differ by only a factor of three ($\rho_l = 740\frac{kg}{m^3}$ and $\rho_v = 250\frac{kg}{m^3}$). We could not perform a direct calibration of the LVDT at 43K because there was no direct access to the LVDT within the cryostat; however, as shown by Reichenauer and Scherer[8,9,24], information can be extracted about the sample shrinkage from the adsorption isotherm itself.

Since capillary condensation occurs over a narrow pressure range ($0.998 < \frac{P}{P_0} < 1$), the liquid can be treated as incompressible during capillary condensation. The high density corners of the adsorption and desorption isotherms (points "B" and "D" in Fig. 1a respectively) correspond to the aerogel being full of liquid, but compressed because of capillary forces at the surface pores. After capillary condensation was complete in this sample, the aerogel continued to adsorb fluid up until bulk saturation was reached (just below point "C"). The significant

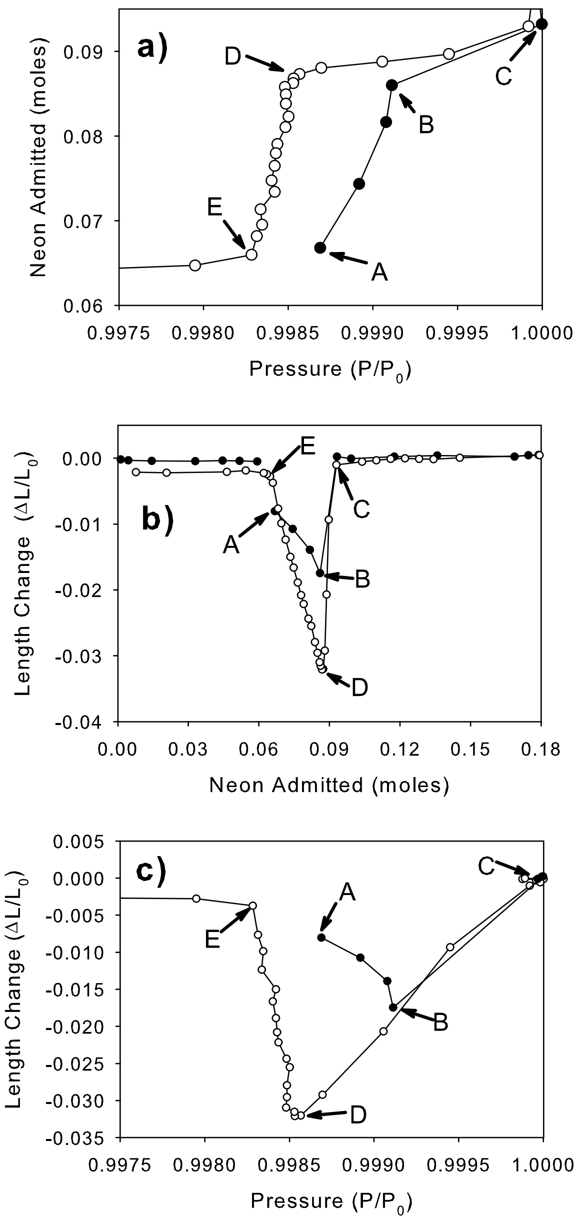

FIG. 1: (a)Adsorption isotherm for neon in B51. (b)Contraction of the aerogel as a function of neon added to cell. (c)Contraction of the aerogel as a function of system pressure. Data were taken during filling (solid symbols) and emptying (open symbols). Points "A" and "B" refer to the beginning and end of capillary condensation during filling. At point "C" the gel is full of liquid but completely relaxed. At point "D" the gel is still full of liquid but the aerogel has been compressed by the removal of some of the neon, so that its pore volume has been reduced. At point "E" the aerogel is empty of liquid, but shows permanent deformation.

slope of the isotherm between capillary condensation and bulk condensation (i.e. $0.999 < \frac{P}{P_0} < 1$) indicates that the aerogel was still adsorbing liquid even though there was no longer any vapor within the pores. By measuring how much fluid was adsorbed after the completion of capillary condensation it is possible to calculate how much swelling occurred in the aerogel over this pressure range. The degree of swelling can then be used to form a calibration for the LVDT.

The bulk neon vapor at 43K has a high density and the cell included a large bulk volume, so the total amount of neon admitted into the cell does not correspond to the amount of neon adsorbed by the aerogel. However, since we are dealing with such a small pressure range during capillary condensation we can assume that all neon admitted over the pressure range $0.999 < \frac{P}{P_0} < 1$ is adsorbed by the aerogel – the bulk vapor density changes very little over this range.

Assuming the deformation of the aerogel is isotropic, the change in aerogel volume (ΔV) can be related to the change in its length (ΔL) and the quantity of fluid (Δn) adsorbed during swelling (or shrinking) by:

$$\Delta V = \frac{\Delta n}{\rho_l - \rho_v} = V_0 \left[1 - \left(1 - \frac{\Delta L}{L_0}\right)^3\right] \qquad (1)$$

where "L_0" and "V_0" are the initial length and volume of the aerogel sample and "ρ_l" and "ρ_v" are the density of liquid and gaseous neon respectively. While this technique is not very precise, it does give an estimate of the maximum linear aerogel compression which can then be used as an LVDT calibration.

Using this calibration the aerogel length change has been plotted as a function of the amount of neon adsorbed in Fig. 1b and as a function of pressure in Fig. 1c. Zero has been set to be the fully relaxed aerogel filled with liquid. Within the resolution of the LVDT no deformation was seen for the first 0.06 moles of neon admitted to the cell — in this regime, a thin film was collecting on the aerogel strands in equilibrium with bulk vapor. Then, as neon began to capillary condense near point A, the aerogel contracted reaching a maximum linear compression of almost 2% at point B. At this point the gel was full of liquid, but compressed from its original volume. As more neon was added to the cell it was adsorbed by the aerogel, allowing the gel to relax and expand. Once the gel was full and bulk liquid began collecting (at point C, $n_{neon} \sim 0.095$moles), there were no longer any curved liquid-vapor interfaces causing stress within the aerogel and it had re-expanded to its original size. Upon desorption of the neon, the process occurred in reverse; however during desorption the aerogel was linearly compressed by almost 3.5% at point D. By point E the aerogel had re-expanded — in this pressure regime only a film of neon remains on the silica strands. However, the gel did not fully return to its original size; there was a slight permanent deformation (about 0.2% linear compression).

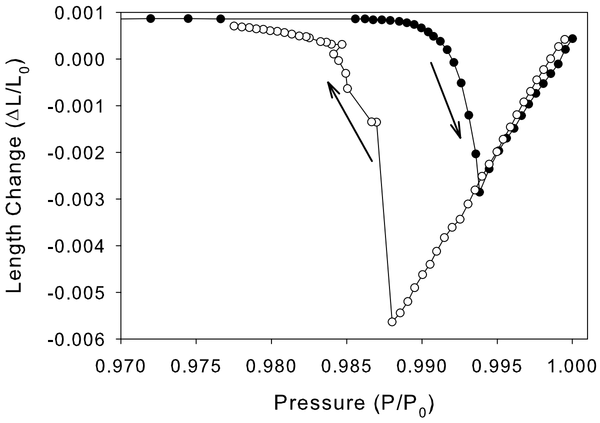

FIG. 2: Deformation of B110 during adsorption (solid symbols) and desorption (open symbols) of helium at 4.2K.

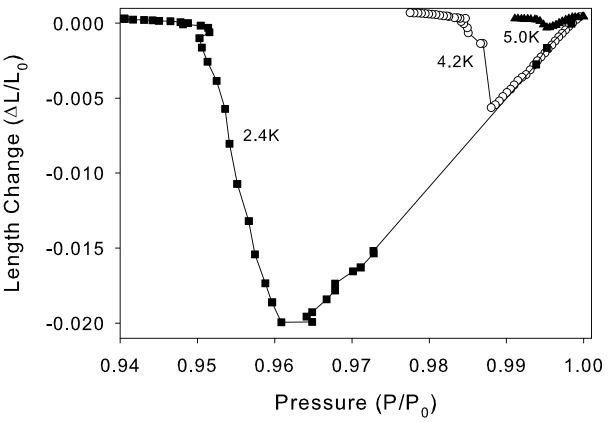

FIG. 3: Deformation of B110 during emptying isotherms at 2.4K, 4.2K, and 5.0K.

Hysteresis is generally observed for adsorption of fluids in porous media — the adsorption and desorption of the fluid taking place at different partial pressures. The precise mechanism of this hysteresis is an open question for aerogels, but it may indicate a different liquid-vapor interface shape for adsorption and desorption. The lower partial pressure for desorption means that there exists a greater pressure difference across the curved liquid-vapor interface, and results in a greater maximum stress on the aerogel during desorption.

The portion of the isotherms closest to P_0 are identical for the emptying and filling branches of the isotherm; in this region the gel is full of liquid and the aerogel matrix is swelling or shrinking in response to the pressure difference across the liquid-vapor interface present at the aerogel surface rather than interfaces within the pores.

IV. HELIUM IN AEROGEL B110

The second experimental cell, used to investigate helium adsorption in aerogel, allowed more precise compression and pressure measurements. It also allowed a direct low temperature calibration for the LVDT. The LVDT calibration was reproducible to within about 1% upon thermal cycling. Since the sample had a smaller diameter than the B51 sample, the pressure exerted by the weight of the ferromagnetic core was larger. To avoid overloading the sample we used a denser aerogel, B110, in this cell; the gel was compressed about 0.3% by the weight of the core ($\sim$ 3g).

An isotherm for helium in B110 at 4.200K is shown as Fig. 2. Since the pressure in the cell is controlled rather than the quantity of helium, the isotherm is only plotted with length change as a function of cell pressure, as in Fig. 1c. During the low pressure, $P/P_0 < 0.95$, formation of a thin film of helium the aerogel expanded by about 0.08%. Equilibration took many hours for these films, so equilibrium data of the initial dilation of aerogel upon helium adsorption were not collected. Similar long equilibration times for helium films in aerogels have been observed before, as has the dilation[2]. Equilibration of points within the hysteretic region was also very slow[21]. The maximum contraction occurred during desorption and was equal to about 0.6% of total length.

Figure 3 shows three desorption isotherms taken at 2.4K, 4.2K and 5.0K respectively. As the temperature was raised, the surface tension of the helium decreased, causing less deformation of the aerogel. The maximum deformation decreased by more than a factor of twenty between 2.4K and 5.0K. No permanent compression was observed for this sample. Above the critical temperature of helium (T_c=5.195K) no contraction was observed, as would be expected without a liquid-vapor interface.

V. ANALYSIS/DISCUSSION

A. Dilation at low vapor pressure

Consistent with an earlier study[2], dilation of the aerogel during the initial stages of helium adsorption was observed at all temperatures studied. The maximum dilation depended much less on temperature than did the deformation during capillary condensation — in all cases it was just under 0.1% of the total sample length. This is consistent with the dilation being governed by the energetics of adsorption sites on the silica strands, which can involve binding energies much larger the liquid-vapor interfacial energy or the thermal energy at liquid helium temperatures.

B. Aerogel bulk modulus

During fluid adsorption and desorption, curved liquid-vapor interfaces abound within the open aerogel pore structure. A Laplace pressure exists across each of these interfaces, which can place stress on the aerogel. The Laplace pressure is a purely mechanical construct, with the surface tension (σ_{lv}) across the interface responsible for the pressure difference between the liquid (P_l) and vapor (P_v) phases:

$$\Delta P \;=\; P_l - P_v \;=\; \frac{2\sigma_{lv}}{r} \tag{2}$$

assuming a hemispherical interface or radius r. Usually the porous medium is assumed to be rigid, but aerogels are extraordinarily compliant, and any stresses must be balanced by deformation of the aerogel. Once the aerogel is completely filled with liquid, the liquid-vapor interface exists only at the aerogel surface and the Laplace pressure is felt as a macroscopic stress.

The Laplace pressure also results in undersaturation — the condensation of fluids below bulk saturation pressure (P_0). This behavior is described by the Kelvin equation, which can be expressed in many forms. The simplest form for our purposes[25] relates the stress caused by the fluid interface to the vapor pressure in the cell:

$$P_l - P_v = \left(\frac{V_v - V_l}{V_l}\right)(P_v - P_0) \tag{3}$$

Here P_l and P_v are the pressures, and V_l and V_v the molar volumes, of the liquid and vapor phases respectively. This derivation assumes that the liquid and vapor are incompressible, which is a fairly accurate approximation given the small pressure ranges over which capillary condensation occurs in aerogels.

When the Laplace pressure acts as a macroscopic stress, then the Kelvin equation can be used to relate the stress on the aerogel to the vapor pressure in the cell. Thus Eq. 3 can be combined with the measured slope of the isotherms after capillary condensation has occurred (e.g. for $0.995 < \frac{P}{P_0} < 1$ for helium in B110 at 4.2K) to calculate the elastic properties of the aerogel. In this regime the gel was full of liquid and the pressure difference between the liquid and vapor phases was balanced by the elastic stress of the aerogel. If the deformation of the aerogels is isotropic then the bulk modulus, K$_{gel}$, can be used to characterize its response to the stress exerted by the liquid-vapor interface.

For high porosity aerogels and small deformations (i.e. $\frac{\Delta L}{L_0} \approx \frac{\Delta V}{3V_0}$) the sample experiences this pressure difference as a compressive stress, which gives:

$$\frac{\Delta L}{L_0} \approx \frac{1}{3}\frac{1}{K_{gel}}\left(\frac{V_v - V_l}{V_l}\right)(P_v - P_0) \tag{4}$$

Thus we can extract a value for K$_{gel}$ from the slope of each isotherm when plotted as $\Delta L/L_0$ *vs* P_v, without needing to know either the fluid's surface tension or the aerogel's pore size. In fact, measurements on this portion of our isotherm, where the aerogel is full but partially compressed, cannot tell us about the effective pore size. That information (R$_{cap}$) comes from the "breakthrough radius," the point at which the meniscus curvature r becomes equal to an effective pore size during desorption and the interface becomes unstable so that the pores suddenly empty.

If we know the liquid's surface tension and the pressure, P_v, at which pores begin to empty, we can determine a pore size, R_{cap}. In fact, this is a standard way of determining pore size from isotherms — there is no need to measure sample deformation ΔL, the desorption pressure is all that is necessary. Assuming the simplest (hemispherical) form for the meniscus, then at breakthrough:

$$(P_0 - P_v) = \left(\frac{V_l}{V_v - V_l}\right)\frac{2\sigma_{lv}}{R_{cap}} \tag{5}$$

A similar calculation can define a radius during adsorption, although its meaning is less clear.

This derivation assumes that the liquid and vapor are incompressible, which is a fairly accurate approximation given the small pressure ranges over which capillary condensation occurs in aerogels. More commonly one assumes the vapor behaves like an ideal gas and the liquid molar volume is much smaller and can be neglected. This gives the more familiar form of the Kelvin equation:

$$-RT\ln\frac{P_v}{P_0} = -V_l\frac{2\sigma_{lv}}{r} + V_l(P_0 - P_v) \tag{6}$$

Neither of these assumptions is appropriate near the liquid-vapor critical point, so we use the form in Eq. 5 rather than Eq. 6.

What our aerogel pore size analysis (from the "breakthrough" pressure, P_v) does is show that this rather macroscopic, classical treatment is valid over a wide range of σ_{lv} near T$_c$ (i.e. the value for R_{cap} is essentially the same, even though σ_{lv} varies by nearly twenty times). This also shows that, despite their unique tenuous structure, quite unlike an array of uniform pores, a description of capillary condensation in terms of a single effective pore size seems adequate.

The bulk moduli calculated from several helium adsorption isotherms in B110 are plotted in Fig. 4. Calculations were made using all adsorption and desorption isotherms separately over a temperature range where σ_{lv} changes by a factor of eighteen, confirming the validity of Eq. 4. The values extracted for K$_{gel}$ are roughly constant, and the mean value (K$_{gel}$ ≈ 0.43MPa) has been included on the plot as a solid line.

The bulk modulus for silica aerogel depends sensitively on aerogel density, and can be extracted from measurements of the Young's modulus (E)[26] or shear modulus (G)[27] using:

$$K = \frac{E}{3(1-2\nu)} = \frac{2(1-\nu)G}{3(1-2\nu)} \tag{7}$$

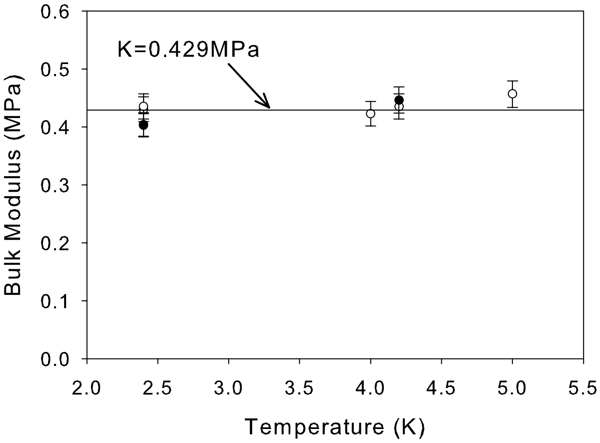

FIG. 4: The bulk modulus of aerogel B110 as calculated from adsorption (solid symbols) and desorption (open symbols) isotherms using Eq.4.

These equations require knowledge of the Poisson's ratio (ν) for aerogel, which is about 0.2[28]. Pure silica has a bulk modulus of roughly 3.5×10^4MPa, much larger than aerogel. The moduli for base catalyzed silica aerogels with densities used in this study ($51\frac{kg}{m^3}$ and $110\frac{kg}{m^3}$) should be about 0.08MPa and 0.8MPa respectively, although these values can vary greatly between samples. Our value for the bulk modulus of B110 of 0.43MPa is consistent with these values, although it is a little lower than expected. A similar calculation for the data in Fig. 1 yields a bulk modulus of K=0.065MPa for aerogel B51.

C. Maximum deformation

Since helium adsorption isotherms in B110 were collected at several temperatures, the temperature dependence of the maximum compression during capillary condensation could be analyzed; Fig. 5 shows the degree of compression during capillary condensation, as well as the bulk surface tension at each temperature. While the degree of contraction depends sensitively on temperature, it scales roughly with surface tension (plotted as a solid line in Fig. 5.

The scaling of maximum deformation with surface tension is consistent with a characteristic "breakthrough radius" describing the curvature of the liquid-vapor interface at the surface of the aerogel just prior to the percolation of the vapor phase into the sample (invasion of the helium vapor phase into aerogel during desorption has been observed[29] in optical experiments). While it is not clear how this breakthrough radius relates to the aerogel structure, the magnitude of this breakthrough radius can be estimated from the desorption isotherm using the Kelvin Equation. A similar calculation can be performed using the pressure at which capillary condensation is complete along the adsorption isotherms, although the form of the liquid-vapor interface during filling is even less clear. Table I summarizes the values of the interface radii calculated from our isotherms, as well as the effective capillary pressure and predicted compression of the aerogels.

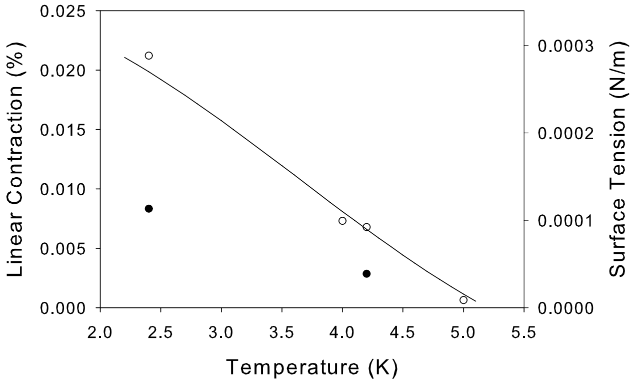

FIG. 5: The amount that sample contracted during adsorption (solid symbols) and desorption (open symbols) is shown here as a function of temperature. The temperature dependence scales roughly with helium surface tension (which is nearly linear in this temperature range), shown as a solid line for comparison.

The capillary pressure generated by the curved liquid-vapor interface during desorption is significant compared to the bulk moduli of the aerogels. It is easy to see how higher surface tension fluids can easily damage aerogels — assuming a breakthrough radius of 20nm, water (295K) and liquid nitrogen (77K) would generate capillary pressures of 7MPa and 0.9MPa respectively, much larger than the bulk moduli of these aerogels.

D. Damage to aerogels

No permanent densification was seen in our denser aerogel (B110) over the range of this experiment. The maximum volumetric compression at any time was about 6%, which is generally within the elastic regime for aerogels. However, B51 appeared to exhibit damage after desorption of neon. It had experienced a 10% volumetric compression, enough to cause permanent structural changes in the aerogel. The manner in which the maximum compression scales with surface tension allows us to predict the compression for a given aerogel, fluid, and temperature. This is especially important for very low density gels, with their associated low bulk moduli — for such samples permanent damage could result from the surface tension of liquid helium. At common filling temperatures, such as 4.2K, gels with porosities or 98% or more will likely be damaged.

Compression of aerogels at room temperature leads to

	B51 – Neon	**B110 – Helium**		
	(43K)	(2.4K)	(4.2K)	(5.0K)
Breakthrough radius, Desorption (nm)	40(4)	21(1)	22(1)	20(1)
"Breakthrough radius," Adsorption (nm)	68(7)	N/A	44(4)	N/A
Surface tension (σ_{lv}) $\left(\frac{mN}{m}\right)$	0.13	0.27	0.090	0.015
Capillary pressure ($P_{cap} = 2\sigma_{lv}/R_{Des}$) (MPa)	0.0064	0.026	0.0082	0.0015
Calculated Bulk Modulus (K_{gel}) (MPa)	0.065	0.43	0.43	0.43
Measured volumetric compression	9%	6%	2%	0.2%

TABLE I: Liquid-vapor interface radii at completion of capillary condensation (or beginning of capillary evaporation) calculated using the Kelvin equation, for adsorption and desorption isotherms shown in this paper. Errors in the last digit are given in parentheses. Also the effective capillary pressures acting on the samples at breakthrough, aerogel bulk moduli, and maximum volumetric contraction during desorption.

bulk densification and important microstructural changes in the sample. Such changes have been investigated[10,11] during the room temperature densification of silica aerogels in a mercury porosimeter. Three characteristics of the aerogel structure were measured — the fractal dimension, the solid particle size, and the cluster size (or correlation length). As the aerogel was compressed the particle size remained unchanged, consistent with the silica particles (that compose the aerogel strands) being relatively unaffected by small pressures. However, the fractal dimension of the aerogels increased slightly, and the correlation length decreased significantly, during compression. These three factors are all very important in determining how fluids are affected by the presence of aerogel, and they are usually assumed to remain constant throughout an experiment. However, if the aerogel is compressed during the experiment these factors may change.

The increase in aerogel density is generally assumed to be due to the preferential collapse of the largest "pores," with relatively little damage to the smallest scale structures. However, the presence of large, open, pores is what distinguishes aerogel from other porous media and any damage to this structure may have dramatic effects on the behavior of fluids within the aerogels. To avoid such damage, one must be careful to avoid capillary stresses that could deform the gel beyond its elastic limit. The safest way to fill or empty an aerogel is above the liquid-vapor critical point, where no liquid-vapor interface exists. However, using calculations such as those shown in Table I allows one to estimate the degree of deformation induced during filling and emptying at lower temperatures, and a filling temperature can be chosen that does not allow the sample to experience plastic deformation.

E. Shape of adsorption isotherms

Note that the amount of neon adsorbed or desorbed at 43K during capillary condensation — the steepest portion of the curve at $P/P_0 \sim 0.9990$(adsorption) or 0.9983(desorption) — is about 65% of the total neon within the gel. The volumetric compression of the aerogel by about 10% during desorption is a significant portion of this, so that compression is a very important part of the capillary condensation behavior. Qualitatively the effect of aerogel compliance is to make the capillary condensation/desorption portions smaller (i.e. the fluid density change from point A to point B in Fig. 1 would be spread out over a wider range, from point A to point C if the aerogel was rigid). Simultaneously, the isotherms become steeper in a compliant material like aerogels since effective pore radius decreases during compression (by up to 3.5%).

VI. SUMMARY

We have investigated the effect of small capillary pressures on the deformation of low density silica aerogels during adsorption and desorption of fluids. For most conditions in this study, this deformation was found to be completely elastic, but in the lower density aerogel (B51) permanent damage was seen. The compression of the aerogel during adsorption and desorption can be used to compute the bulk modulus of the aerogel, with no knowledge of the aerogel pore structure being necessary.

The highly compliant nature of low density aerogels also has important implications for the shape of their adsorption isotherms. This effect becomes less important as the degree of compression is reduced — it is not very significant in the helium adsorption/desorption isotherms in B110. This effect may be further reduced if the aerogel is not free to deform, such as when grown within the small pores of a metal sinter.

Finally, it should be pointed out that when low density silica aerogels are used as a method to introduce disorder into fluid systems such as helium or liquid crystals the aerogels may be damaged by any fluid interfaces present. Even the low surface tensions of ^{3}He and ^{4}He are capable of damaging low density aerogels during filling and emptying.

---

[*] therman@phys.ualberta.ca

[1] R. Beaume, J. Suzanne, and J. G. Dash, Surface Science **92**, 453 (1980).

[2] P. Thibault, J. J. Préjean, and L. Puech, Physical Review B **52**, 17491 (1995).

[3] D. J. C. Yates, Proceedings of the Royal Society of London. Series A **224**, 526 (1954).

[4] T. Takamori and M. Tomozawa, Journal of the American Chemical Society **65**, C127 (1982).

[5] G. W. Scherer, Journal of the american Ceramic Society **69**, 473 (1986).

[6] G. Dolino, D. Bellet, and C. Faivre, Physical Review B **54**, 17919 (1996).

[7] H.-S. Ma, J.-H. Prévost, and G. W. Scherer, International Journal of Solids and Structures **39**, 4605 (2002).

[8] G. Reichenauer and G. W. Scherer, Colloids and Surfaces a — Physicochemical and Engineering Aspects **187**, 41 (2001).

[9] G. Reichenauer and G. W. Scherer, Journal of Non-crystalline Solids **2777**, 162 (2000).

[10] I. Beurroies, L. Duffours, P. Delord, T. Woignier, and J. Phalippou, Journal of Non-crystalline Solids **241**, 38 (1998).

[11] T. Woignier, L. Duffours, I. Beurroies, J. Phalippou, P. Delord, and V. Gibiat, Journal of Sol-Gel Science and Technology **8**, 789 (1997).

[12] J. Shen and P. A. Monson, Molecular Physics **100**, 2031 (2002).

[13] K. Matsumoto, J. V. Porto, L. Pollack, E. N. Smith, T. L. Ho, and J. M. Parpia, Physical Review Letters **79**, 253 (1997).

[14] J. V. Porto and J. M. Parpia, Physical Review B **59**, 14583 (1999).

[15] M. H. W. Chan, K. I. Blum, S. Q. Murphy, G. K. S. Wong, and J. D. Reppy, Physical Review Letters **61**, 1950 (1988).

[16] J. Yoon, D. Sergatskov, J. Ma, N. Mulders, and M. H. W. Chan, Physical Review Letters **80**, 1461 (1998).

[17] M. H. W. Chan, N. Mulders, and J. D. Reppy, Physics Today **49**, 30 (1996).

[18] S. B. Kim, J. Ma, and M. H. W. Chan, Physical Review Letters **71**, 2268 (1993).

[19] N. Mulders and M. H. W. Chan, Physical Review Letters **75**, 3705 (1995).

[20] T. Bellini, L. Radzihovsky, J. Toner, and N. A. Clark, Science **294**, 1074 (2001).

[21] T. Herman, J. Day, and J. Beamish, *arXiv:physics.cond-mat/0505430* (2005).

[22] G. Poelz and R. Riethmüller, Nuclear Instruments and Methods **195**, 491 (1982).

[23] G. C. Straty and E. D. Adams, Review of Scientific Instruments **40**, 1393 (1969).

[24] G. Reichenauer, Particle and Particle Systems Characterization **21**, 117 (2004).

[25] L. D. Landau and E. M. Lifshitz, *Statistical Physics* (Pergamon Press, 1958), chap. 15.

[26] T. Woignier and J. Phalippou, Journal de Physique (Paris) **50**, C4179 (1989).

[27] D. R. Daughton, J. MacDonald, and N. Mulders, Physica B **329-333**, 1233 (2003).

[28] J. Gross, G. Reichenauer, and J. Fricke, Journal of Physics D: Applied Physics **21**, 1447 (1988).

[29] T. Lambert, C. Gabay, L. Puech, and P. E. Wolf, Journal of Low Temperature Physics **134**, 293 (2004).

[30] The neon data were collected using hand wound coils; the helium data were collected using a Schevitz HR050 sensor, available from Measurement Specialties, Inc.. The LVDT output was measured using an LR400 mutual inductance bridge, from Linear Research Inc.

[31] Mensor 1000psi gauge, Model 4040